Inverse Techniques for the Design and Control of Solidification and Forming Processes

Nicholas Zabaras
Sibley School of Mechanical and Aerospace Engineering
188 Frank H. T. Rhodes Hall
Cornell University
Ithaca, NY 14853–3801

ABSTRACT: Almost ten years ago and with the technical and financial support from Alcoa Laboratories and Dr. Owen Richmond, we initiated a research effort in the design of solidification and bulk forming processes. In the front of solidification process design, we have developed inverse techniques for the design of stable solidification growth with desired growth velocity, whereas in the design of forming processes, a continuum sensitivity analysis has been developed for die, preform and process parameter design. We will here briefly review these activities as well as discuss some directions for future research in material process design and control.

1 INVERSE PROBLEMS FOR SOLIDIFICATION DESIGN

The need to design solidification processes that result in a desired thermal field near the solidification front is addressed in Flemings (1974) and posed as an inverse problem in Zabaras et al. (1988, 1992, 1993, 1995a,b) and Kang and Zabaras (1995). After these initial research efforts in one- and two- dimensional design Stefan problems, our work on solidification processing has focused on the development of computational techniques that can be used to design and control the developed microstructures in directional alloy solidification processes.

Gravity plays an important role in the obtained microstructures mainly by affecting the melt flow mechanisms as well as the solute diffusion processes. Since these effects remain present even under a reduced gravity environment, a number of inverse convection design solidification problems was addressed that result in desired freezing front motions and heat fluxes in the solidification of pure materials (Zabaras et al. 1995, 1997 and Yang and Zabaras 1998a).

This work was recently extended to alloy solidification processes where double diffusive mechanisms have to be accounted for in the inverse analysis. Our main design variables are the thermal mold/furnace conditions. We selected these continuous variables such that a desired growth velocity $\mathbf{V}$ and temperature field (e.g. a temperature gradient G) are achieved near the freezing interface that correspond to desired microstructures (Yang and Zabaras, 1998b). In our preliminary work, we are interested to design processes with spatially uniform growth velocity under stable growth conditions.

These design problems are posed as inverse problems with overspecified thermal conditions (temperature and flux) on one part of the boundary (here the freezing interface) and no-thermal conditions on another part of the boundary (here part of the mold or furnace walls). Such problems are mathematically stated as functional optimization problems in the L_2 space. The exact gradient of the cost functional is obtained via the solution of an adjoint continuum problem. A sensitivity problem is also defined and is used in the implementation of the conjugate gradient method. Considering the rapidly changing with respect to time optimum boundary heating/cooling rates for such designed processes, it is important to avoid finite discretization of the boundary heat flux conditions in particular when a-priori information on the type of expected flux solution is not available. In addition, due to the ill-posedness of these inverse problems, time sequential solution is not always possible and spatial and temporal regularization is required when such techniques are employed (Zabaras et al. 1992). However, in the total time domain approach, a-priori information and spatial regularization are not essential (Kang and Zabaras 1995).

Since electromagnetic fields have a direct effect on the strength of the melt flow (Series and Hurle, 1991), it is feasible to consider that the presence of electromagnetic fields facilitates the process of control via thermal boundary heating/cooling. Furthermore, the consideration of designing appropriate strengths and direction of magnetic fields simultaneously with continuous boundary heating/cooling conditions for various strengths of gravity will further enhance the success of the solidification design process.

Finally, real time control of directional processes based on the design methodology reviewed above requires the development of reduced order models (i.e. models with only a few parameters that can be used with minimum CPU requirements). Minimum research has been performed in this area. The significant recent advances in robust control theory (Zhou et al. 1996) can be applied to the development of such controllers and to the real time feedback solidification process control.

1.1 Inverse Design of Alloy Solidification Processes

A review is given here of the design of stable binary alloy solidification processes with desired freezing front motions. It is quite well known that in a binary alloy solidification process, a solute pile-up takes place ahead of the moving interface (Kurz and Fisher 1989). Due to this effect, a region of *constitutional undercooling* (i.e. a region where the actual temperature is less than the local equilibrium temperature) can develop in front of the freezing interface. This leads to interface instability and consequent formation of dendrites. The condition for avoiding such an effect is given in Kurz and Fisher (1989) by the very simple *constitutional stability criterion*,

$$\frac{\partial \theta}{\partial n}(\boldsymbol{x},t) < m\,\frac{\partial c}{\partial n}(\boldsymbol{x},t), \quad (\boldsymbol{x},t) \in \Gamma_I \times [0, t_{max}] \quad (1)$$

where $G \equiv \frac{\partial \theta}{\partial n}(\boldsymbol{x},t)$ and $G_c \equiv \frac{\partial c}{\partial n}(\boldsymbol{x},t)$ are the temperature and concentration gradients at the interface with the direction of the unit normal vector to the freezing interface pointing into the solid phase.

In the work of Yang and Zabaras (1998b), this inequality condition was converted to an equality form as follows:

$$\frac{\partial \theta}{\partial n}(\boldsymbol{x},t) = m\frac{\partial c}{\partial n}(\boldsymbol{x},t) + \epsilon(\boldsymbol{x},t) \quad (2)$$

where the *over stability function* $\epsilon(\boldsymbol{x},t), (\boldsymbol{x},t) \in \Gamma_I \times [0, t_{max}]$, is non-positive and is a part of the inverse problem definition. The above approach has been applied in our recent work.

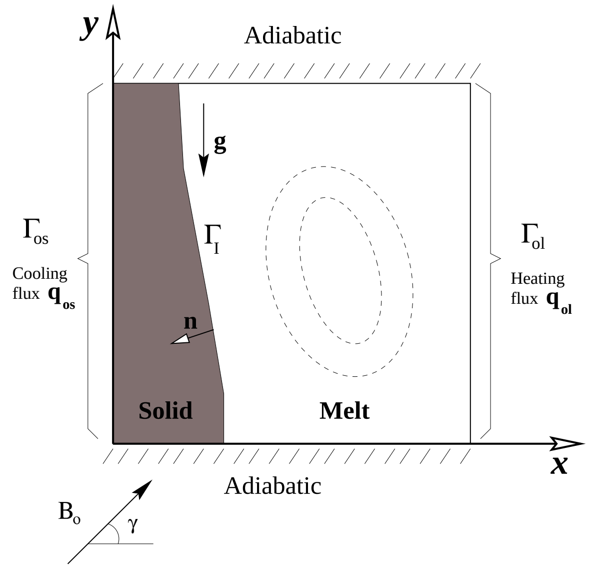

Figure 1: Schematic of the direct alloy solidification problem in the presence of a magnetic field.

It is assumed that there is enough regularity of the boundary to allow us to work in the framework of $H^1(\Omega)$ functions. The space of *admissible controls* $\mathcal{U}$ is next defined as the Hilbert space $\mathcal{U} = L_2(\Gamma_{ol} \times [0, t_{max}])$. The inverse design magneto-thermo-solutal convection problem in the liquid phase can now be formulated as a whole time-domain optimization problem. With the following *guessed* heat flux condition at the liquid boundary mold wall:

$$\frac{\partial \theta}{\partial n}(\boldsymbol{x},t) = q_{ol}(\boldsymbol{x},t), \quad (\boldsymbol{x},t) \in \Gamma_{ol} \times [0, t_{max}] \quad (3)$$

one can define a direct thermo-solutal convection problem (in the presence of a magnetic field) on a prescribed variable domain $\Omega_l(t)$. For the definition of this parametric direct problem, the following boundary conditions are used at the freezing interface: (a) the stability condition (equ. (2)),

(b) the solute balance conditions, (c) the given desired interface velocity and (d) the zero flux of the electric potential ϕ (Sampath and Zabaras 1999b).

Let us denote the solution of this direct problem for the electric potential, temperature, concentration and flow fields as $\phi(\boldsymbol{x}, t; q_{ol})$, $\theta(\boldsymbol{x}, t; q_{ol})$, $c(\boldsymbol{x}, t; q_{ol})$ and $\boldsymbol{v}(\boldsymbol{x}, t; q_{ol})$, respectively, indicating their parametric dependence on q_{ol}.

The liquidus relation from the equilibrium phase diagram is not used in the above *direct problem* definition, thus it is not guaranteed to be satisfied. Instead, for arbitrary $q_{ol} \in \mathcal{U}$, we define the following cost functional in the space $L_2(\Gamma_I \times [0, t_{max}])$:

$$J(q_{ol}) = \frac{1}{2} || \theta(\boldsymbol{x}, t; q_{ol}) - (\theta_m + mc(\boldsymbol{x}, t; q_{ol})) ||^2 \quad (4)$$

The above functional indicates the discrepancy of the calculated temperature from the concentration-dependent liquidus temperature. This discrepancy can be thought of as a measure of the deviation of the interface from the thermodynamic equilibrium conditions for the dilute binary alloy. Finally, the following *control problem* is defined:

Find $\bar{q}_{ol} \in \mathcal{U}$ *such that*

$$J(\bar{q}_{ol}) \leq J(q_{ol}), \qquad \forall \; q_{ol} \; \in \; \mathcal{U} \quad (5)$$

The objective of the inverse analysis is then to construct a minimizing sequence $q^k_{ol}(\boldsymbol{x}, t) \;\; \in \mathcal{U}$, $k = 1, 2, \ldots$ that converges to at least a local minimum of $J(q_{ol})$ (Fletcher 1987). If such a minimum can lead to an interface growth that is close enough to the desired growth according to a certain accuracy measure and is constitutionally stable, then an acceptable design solution has been obtained.

The main difficulty with the above optimization problem is the calculation of the gradient $J'(q_{ol}(\boldsymbol{x}, t))$ in the space $\mathcal{U}$. Taking the directional derivative of the cost functional at q_{ol} in the direction Δq_{ol}, yields the following equation:

$$D_{\Delta q_{ol}} J(q_{ol}) \equiv (J'(q_{ol}), \Delta q_{ol})_{\mathcal{U}} =$$

$$(\Theta(\boldsymbol{x}, t; q_{ol}, \Delta q_{ol}) - mC(\boldsymbol{x}, t; q_{ol}, \Delta q_{ol}),$$

$$\theta(\boldsymbol{x}, t; q_{ol}) - (\theta_m + mc(\boldsymbol{x}, t; q_{ol})))_{\Gamma_I} \quad (6)$$

where $\Theta(\boldsymbol{x}, t; q_{ol}, \Delta q_{ol})$ is the linear sensitivity temperature field. The sensitivity temperature field $\Theta(\boldsymbol{x}, t; q_{ol}, \Delta q_{ol}) \equiv D_{\Delta q_{ol}} \theta(\boldsymbol{x}, t; q_{ol})$, the sensitivity velocity field $\mathbf{V}(\boldsymbol{x}, t; q_{ol}, \Delta q_{ol}) \equiv D_{\Delta q_{ol}} \boldsymbol{v}(\boldsymbol{x}, t; q_{ol})$, the sensitivity concentration field $C(\boldsymbol{x}, t; q_{ol}, \Delta q_{ol}) \equiv D_{\Delta q_{ol}} c(\boldsymbol{x}, t; q_{ol})$ and the sensitivity electric potential field $\Phi(\boldsymbol{x}, t; q_{ol}, \Delta q_{ol}) \equiv D_{\Delta q_{ol}} \phi(\boldsymbol{x}, t; q_{ol})$ together constitute a *linear continuum magneto-thermo-solutal sensitivity problem.* A linear perturbation of the direct magneto-thermo-solutal problem defined leads to the corresponding sensitivity problem. As can be seen from equ. (6), an adjoint system has to be evaluated for the calculation of $J'(q_{ol})$. This adjoint problem is also a linear coupled magneto-thermo-solutal convection problem. A precise definition and derivation of the direct, sensitivity and adjoint problems can be found in (Sampath and Zabaras 1999b).

The application of an external magnetic field has positive effects on both the solutal variation as well as the melt flow in the solidification system. However, the application of a magnetic field alone does not ensure constitutionally stable growth through out the process even though it provides an improvement over the case with no magnetic field. However, simultaneous application of magnetic field and thermal control can lead to improved thermal boundary flux profiles as well as desirable solute segregation patterns (Sampath and Zabaras 1999b). In our recent calculations, the inverse design methodology has been utilized to design a stable growth process with a growth velocity corresponding to that of a solidification process controlled only by heat and solute diffusion.

1.2 Future directions in solidification process design and control

Over a period of ten years, our research has moved from conduction based inverse Stefan models to double-diffusive inverse convection problems in the presence of magnetic fields. Even though some applications to solidification design have been considered in this area, several challenging problems remain to be investigated. We here discuss some of the open research issues in solidification process design and control:

- Issues of uniqueness, existence and stability of solution of general inverse convection problems have only been investigated numerically and a rigorous mathematical approach is not available.

- The solution of design solidification problems is not directly useful for real time control of solidification processes. Model reduction techniques are needed using the information provided by the continuum design techniques. Many interesting and exciting problems are to be addressed in this area and the significant developments in robust control theory are expected to be directly applicable to such problems.

- Consideration of other than the simplistic constitutional undercooling criterion is needed to be incorporated in the definition of the design problem for a stable desired growth. This will introduce mathematical difficulties in obtaining the desired adjoint operators. Also, additional physical mechanisms may also have to be considered (e.g. surface tension, interface kinetics, etc.) (Coriell and McFadden 1994).

- Current work is underway for the optimum design of external magnetic fields (magnitude and direction) that in addition to the controlled boundary heating/cooling rates can be used to achieve the desired objectives in the freezing front or the final cast product. Consideration of the full set of coupled PDEs for the electromagnetics is still an active research area with regard to direct modeling and as such even further work remains to be considered in an inverse analysis.

- Consideration of rotation of the crucible or furnace in addition to boundary fluxes and magnetic fields provides another means for controlling the obtained solidification microstructures. While a lots of experimental work and data are available in this topic, no research as of yet has been initiated for the inverse design of solidification systems via rotation.

- Most of the current developments on design solidification problems are for stable solidification growth. However, there are many other important design problems in the solidification of alloys with diffused (mushy) interfaces that remain to be addressed (Zabaras 1998). For such alloy solidification problems, one may consider the problem of minimizing macrosegregation (uniformity in c in the final product) or obtaining a product with a stratified distribution of concentration. Many difficulties exist in this area mainly related to insufficient understanding and modeling of mushy zones that will allow us to perform a rigorous mathematical analysis for the inverse design problem.

- Finally, implementation issues of functional optimization problems as applied to the design of solidification processes remain to be addressed. Object oriented techniques have been found efficient for such purposes and they are currently under intensive research (Sampath and Zabaras 1999a,b,c).

- The proposed techniques are useful for the development of the next generation of furnaces for controlled crystal growth. In particular, the availability of mathematical models for solidification control via optimally designed thermal boundary fluxes and electromagnetic fields is essential for the development of multiple zone instrumented furnaces. The need for the development of such furnaces was not addressed up to now mainly because the prospects of controlled solidification processes were not there. In the last several years, it has been shown that the mathematical control of solidification processes is possible and that the time of developing advanced furnaces that can produce the desired heating/cooling boundary fluxes has arrived.

- In addition to applications in the design of solidification processes, the proposed designs can be applied to experimental studies of processes in which the effects of convection on the solidification microstructures are reduced and diffusion based mechanisms are dominant.

From the problems listed above, it is clear that solidification process design and control is an exciting area of research and significant challenges and achievements are expected in the near future.

2 INVERSE PROBLEMS FOR FORMING DESIGN

A significant number of metal alloys is currently employed in the manufacturing of automotive, aerospace and other hardware components. The high cost of manufacturing critical structural components can be significantly reduced with the development of mathematically and physically sound computational methodologies for deformation process design and control. The complicated nature of polycrystalline materials and the induced changes in their microstructure during processing are among the main challenges that one must consider while developing means for the design and control of bulk forming processes that under minimum cost result in products of desired shape and material state.

The desired objectives for a single forming process, e.g. in a hot extrusion process, may include one or more of the following criteria: uniform deformation in the final product; minimum required work or extrusion pressure; desired microstructure in the final product; minimum or desired residual stress distribution; minimum deformation and wear of the die; desired shape of the final product; and minimum porosity in the final product. Any of these objectives can theoretically be achieved by: appropriate design of the extrusion die surface; design of the preform; design of the material state (microstructure) in the initial billet; and appropriate selection of the process parameters (extrusion speed and pressure history, operating temperature, etc.). However, it is important to note that in a single forming process there is only a limited control of the material state in the final product that someone can achieve using a single process design and generally a multistage process design is required.

Most deformation process design is currently focused on trial and error techniques based on previous experience and the results of the direct analysis (Kobayashi et al. 1989). On the other hand, sensitivity analysis and optimization theory, provide a fresh look at these problems and can lead to realistic and accurate designs. To mathematically address forming design problems using optimization theory, one needs to calculate the sensitivity of the material state and geometry at the intermediate and final stages of deformation with respect to infinitesimal changes in each of the design variables.

In the direct differentiation method, a set of field equations are developed by considering the variation of the continuum or discretized field equations of the direct problem with respect to small changes in the design parameters (Kleiber et al. 1997). The sensitivity field equations are linear and can easily be solved.

Although the last few years have seen an increasing interest in the direct differentiation method for calculating sensitivities, a number of challenges remain in the accurate and effective computation of sensitivity fields for practical engineering problems that involve frictional contact. Shape optimization schemes for non-steady state metal forming processes with applications to preform forging design are given in (Badrinarayanan et al. 1995, Fourment et al. 1996a,b). Application of optimization techniques for net-shape manufacturing involving forging processes is given in (Zhao et al. 1997). Other applications to extrusion and forging die design can be found in (Badrinarayanan and Zabaras 1996), (Joun and Hwang 1998b) and (Chung and Hwang 1998).

Some of our most recent work in this area is reviewed briefly in the next section and a number of open research issues are discussed in section 2.2.

2.1 Inverse modeling of design forming problems

The work summarized here is an extension of recent work by Zabaras and co-workers (Badrinarayanan and Zabaras 1996, Zabaras and Bao 1999 and Srikanth and Zabaras 1999). The discussion below is restricted to preform design problems and the calculation of sensitivity fields is with respect to the preform shape.

In a typical Lagrangian analysis of a deformation process, material occupying an initial configuration (time zero) is deformed to obtain a final configuration. Since we are interested in the variation of Lagrangian fields induced by a variation in the initial shape of the body, we need to define an imaginary *fixed* geometric configuration which under appropriate smooth geometric mappings is mapped to each of the preform shapes. Furthermore, we assume that the material is in its virgin state in its initial configurations defined fom each preform. Thus, we consider the workpiece in the following configurations (see Fig. 2):

- the *reference* configuration: $\boldsymbol{B}_R$.
  $\boldsymbol{Y}$ will denote an arbitrary point in this configuration. The points of this configuration do not have any material significance.

- the *material* initial configuration: $\boldsymbol{B}_0$, at time $t = 0$.

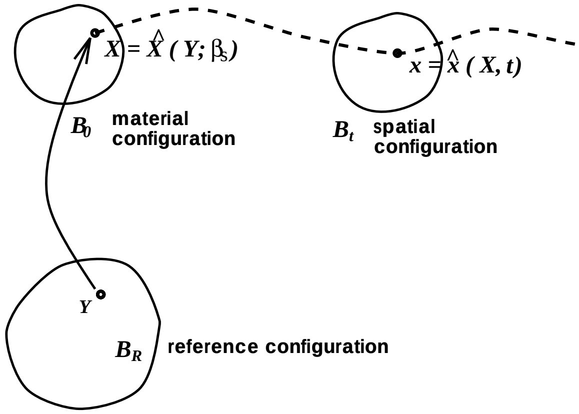

Figure 2: The reference, material and spatial configurations.

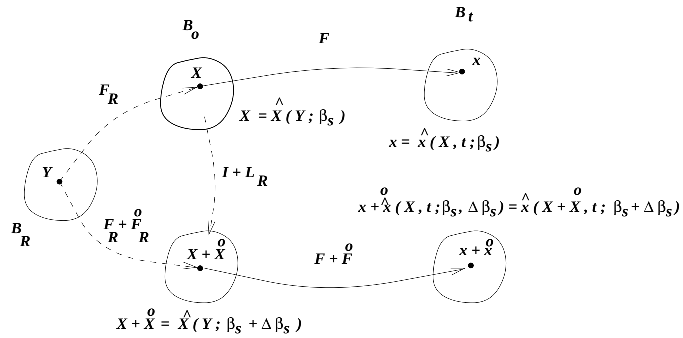

Figure 3: Schematic representation of the shape sensitivity of the deformation.

This configuration represents the initial state of the material that undergoes the deformation process, and the material points of this configuration will be denoted by $\boldsymbol{X}$. The configuration $\boldsymbol{B}_0$ is completely described by a sufficiently smooth *reference map* of the form:

$$\boldsymbol{X} = \hat{\boldsymbol{X}}\left(\boldsymbol{Y}; \beta_s\right) \tag{7}$$

where in general, β_s are smooth functions that define the whole or parts of $\boldsymbol{\partial B}_0$. For a fixed reference configuration $\boldsymbol{B}_R$ and a given boundary of the initial configuration defined through the functions parameters β_s, one can always construct a mapping of the form of equ. (7).

- the *spatial* configuration: $\boldsymbol{B}_t$ at time t.
  This represents the state of the body undergoing deformation through the given die after an elapsed time t. The points in this configurations will be denoted by $\boldsymbol{x}$ and the motion of the body is described with respect to the material configuration by:

$$\boldsymbol{x} = \hat{\boldsymbol{x}}\left(\boldsymbol{X}, t; \beta_s\right) \tag{8}$$

and with respect to the reference configuration by:

$$\boldsymbol{x} = \hat{\boldsymbol{x}}\left(\hat{\boldsymbol{X}}\left(\boldsymbol{Y}; \beta_s\right), t; \beta_s\right) = \tilde{\boldsymbol{x}}\left(\boldsymbol{Y}, t; \beta_s\right) \tag{9}$$

Consider the dependence of Lagrangian fields $\Phi = \hat{\Phi}(\boldsymbol{X}, t)$ on β_s. This dependence can be expressed as follows

$$\Phi = \hat{\Phi}(\hat{\boldsymbol{X}}(\boldsymbol{Y}; \beta_s), t; \beta_s) = \tilde{\Phi}(\boldsymbol{Y}, t; \beta_s) \tag{10}$$

The dependence of Eulerian fields on β_s can easily be derived using equation (9).

The shape differential $\overset{\circ}{\hat{\Phi}} = \overset{\circ}{\hat{\Phi}}\ (\boldsymbol{X}, t; \beta_s; \Delta\beta_s)$ is the total Gateaux differential of $\Phi = \tilde{\Phi}(\boldsymbol{Y}, t; \beta_s)$ in the direction $\Delta\beta_s$ computed at β_s :

$$\overset{\circ}{\hat{\Phi}}\ (\boldsymbol{X}, t; \beta_s, \Delta\beta_s) = \frac{d}{d\lambda}\ \tilde{\Phi}(\boldsymbol{Y}, t; \beta_s + \lambda\Delta\beta_s)\Big|_{\lambda=0} \tag{11}$$

The shape differential or sensitivity $\overset{\circ}{\Phi}$ can be understood as being the difference between two fields representing Φ, that result due to different initial configurations defined by the shape parameters β_s and $\beta_s + \Delta\beta_s$. It is emphasized that the fields $\tilde{\Phi}(\beta_s)$ and $\tilde{\Phi}(\beta_s + \Delta\beta_s)$ are computed for material points that occupy the same location $\boldsymbol{Y}$ in the *fictitious* parent configuration. A graphical representation of the notion of shape sensitivity is shown in Figure 3.

In the remaining of the paper, we will adopt the following notation. While evaluating the spatial derivatives, $\nabla_X \boldsymbol{Z}$ will imply evaluating the gradients for the function $\hat{\boldsymbol{Z}}$ whereas, $\nabla_Y \boldsymbol{Z}$ will denote evaluation of the gradient of the function $\tilde{\boldsymbol{Z}}$.

The shape derivatives of various spatial derivatives with respect to the material configuration $\boldsymbol{B}_0$ have to be evaluated carefully. We first introduce the *reference gradient*, $\boldsymbol{F}_R$, as follows:

$$\boldsymbol{F}_R = \nabla_Y \boldsymbol{X} = \frac{\partial}{\partial \boldsymbol{Y}} \hat{\boldsymbol{X}}\left(\boldsymbol{Y}; \beta_s\right) \tag{12}$$

The shape derivative of the reference gradient, denoted by $\overset{\circ}{\boldsymbol{F}}_R$, is defined as:

$$\overset{\circ}{\boldsymbol{F}}_R = \frac{\partial}{\partial \boldsymbol{Y}}\ \overset{\circ}{\hat{\boldsymbol{X}}}\left(\boldsymbol{Y}; \beta_s\right) \tag{13}$$

We further define $\boldsymbol{L}_R$ as:

$$\boldsymbol{L}_R = \overset{\circ}{\boldsymbol{F}}_R \;\; \boldsymbol{F}_R^{-1} \tag{14}$$

All spatial derivatives with respect to the configuration $\boldsymbol{B}_0$ are expressed in terms of spatial derivatives with respect to the configuration $\boldsymbol{B}_R$ using $\boldsymbol{F}_R$. The calculation of the shape derivatives of these gradients can then be performed in a straight forward manner.

It is here assumed that the direct problem for a given preform defined by the parameters β_s has been solved and the history of deformation, stresses and material state has been evaluated at all times.

Suppose at time step $t = t_n$, we calculated the various direct fields, $(\boldsymbol{T}_n, \sigma_n, s_n, \boldsymbol{F}_n, \boldsymbol{F}^e_n, \bar{\boldsymbol{F}}^p_n)$ as well as the corresponding sensitivity fields $(\overset{\circ}{\boldsymbol{T}}_n, \overset{\circ}{\sigma}_n, \overset{\circ}{s}_n, \overset{\circ}{\boldsymbol{F}}_n, \overset{\circ}{\boldsymbol{F}^e}_n, \overset{\circ}{\bar{\boldsymbol{F}}^p}_n)$. After solving the direct problem at time step $t = t_{n+1}$ and evaluating $(\boldsymbol{T}_{n+1}, \sigma_{n+1}, s_{n+1}, \boldsymbol{F}_{n+1}, \boldsymbol{F}^e_{n+1}, \bar{\boldsymbol{F}}^p_{n+1})$, the *incremental sensitivity problem* is defined as the calculation of the sensitivity fields $(\overset{\circ}{\boldsymbol{T}}_{n+1}, \overset{\circ}{\sigma}_{n+1}, \overset{\circ}{s}_{n+1}, \overset{\circ}{\boldsymbol{F}}_{n+1}, \overset{\circ}{\boldsymbol{F}^e}_{n+1}, \overset{\circ}{\bar{\boldsymbol{F}}^p}_{n+1})$. The discussion here is restricted to isothermal deformation and the rate-dependent material model is defined with one isotropic state variable s as in Weber and Anand (1990) and Zabaras and Srikanth (1999).

The developed continuum sensitivity analysis proceeds in a time incremental fashion using the same time step as in the direct analysis. The incremental sensitivity problem from time t_n to time t_{n+1} is divided in three main subproblems (1) the constitutive sensitivity problem (2) the kinematic sensitivity problem and (3) the contact sensitivity problem. The definition of these problems is given next together with a brief discussion on the current solution techniques and open issues.

The sensitivity constitutive problem

In the constitutive sensitivity problem, one assumes that the sensitivities of the various material state variables, deformation gradient, etc. at time step $t = t_n$, $(\overset{\circ}{\boldsymbol{T}}_n, \overset{\circ}{\sigma}_n, \overset{\circ}{s}_n, \overset{\circ}{\boldsymbol{F}}_n, \overset{\circ}{\boldsymbol{F}^e}_n, \overset{\circ}{\bar{\boldsymbol{F}}^p}_n)$, are given. The material state variables and deformation are assumed known from the direct analysis at both time $t = t_n$ and $t = t_{n+1}$. The objective of the incremental constitutive sensitivity problem at time $t = t_{n+1}$ is the calculation of the linear relationship between the sensitivity fields $(\overset{\circ}{\boldsymbol{T}}_{n+1}, \overset{\circ}{\sigma}_{n+1}, \overset{\circ}{s}_{n+1}, \overset{\circ}{\boldsymbol{F}^e}_{n+1}, \overset{\circ}{\bar{\boldsymbol{F}}^p}_{n+1})$ and the sensitivity of the total deformation gradient $\overset{\circ}{\boldsymbol{F}}_{n+1}$. Note that only a linear relation is calculated here and not the actual sensitivity fields at t_{n+1}.

The sensitivity kinematic problem

In the kinematic sensitivity problem, given $(\boldsymbol{T}_{n+1}, \sigma_{n+1}, s_{n+1}, \boldsymbol{F}_{n+1}, \boldsymbol{F}^e_{n+1}, \boldsymbol{F}^p_{n+1})$ at time $t = t_{n+1}$ and with given linear relationship between $(\overset{\circ}{\boldsymbol{T}}_{n+1}, \overset{\circ}{\sigma}_{n+1}, \overset{\circ}{s}_{n+1}, \overset{\circ}{\boldsymbol{F}^e}_{n+1}, \overset{\circ}{\bar{\boldsymbol{F}}^p}_{n+1})$ and $\overset{\circ}{\boldsymbol{F}}_{n+1}$, and appropriate (e.g. kinematic) sensitivity boundary conditions, one calculates the sensitivity of the deformation gradient $\overset{\circ}{\boldsymbol{F}}_{n+1}$.

After the calculation of $\overset{\circ}{\boldsymbol{F}}_{n+1}$, one can return to the sensitivity constitutive problem and using the various linear relations calculate $(\overset{\circ}{\boldsymbol{T}}_{n+1}, \overset{\circ}{\sigma}_{n+1}, \overset{\circ}{s}_{n+1}, \overset{\circ}{\boldsymbol{F}^e}_{n+1}, \overset{\circ}{\bar{\boldsymbol{F}}^p}_{n+1})$.

The sensitivity contact problem

The objective of this problem is the calculation of the linear relation between the sensitivities of the normal and tangential contact traction components and the sensitivity $\overset{\circ}{\boldsymbol{x}}$ at the contact boundary. Some of the difficulties due to the non differentiable nature of contact are avoided in this calculation by assuming that the same contact boundary exists in both direct problems corresponding to the two nearby preform surfaces (see Fig. 3). This regularizing assumption includes both the sliding and sticking parts of the contact boundary.

The three incremental sensitivity subproblems (constitutive, kinematic and contact) are linearly coupled and together provide a linear problem for the calculation of the sensitivities of both the deformation and the material state. It should be noted that the corresponding subproblems in the direct problem are non-linearly coupled and must be solved in an iterative fashion.

Solution Technique

The solution of the sensitivity constitutive problem is obtained by numerically integrating the sensitivity equations resulting from the linearization with respect to the design variables of the continuum equations describing the material behavior, mainly the flow rule, the evolution of plastic strain, the evolution of state and the elastic law. Very accurate results for such calculations have been reported in our recent work. Note that by differentiating with respect to the preform shape the *continuum* constitutive model, one is able to account for the linearity of the sensitivity fields. Differentiation of the discretized equations, on the other hand, may not lead to the same level of accuracy. This approach implies that the integration scheme for the sensitivity constitutive problem is generally different from that used in the constitutive subproblem of the non-linear direct analysis.

To solve for the sensitivity deformation fields, one needs to consider the sensitivity of the equilibrium equation in conjunction with a set of appropriate boundary conditions. In the following, a principle of virtual work like equation is developed for obtaining $\overset{\circ}{\boldsymbol{F}}$.

The primary unknown in the solution of the sensitivity kinematic problem is the sensitivity of the body configuration $\boldsymbol{x} = \hat{\boldsymbol{x}}(\boldsymbol{X}, t)$. For a sensitivity formulation expressed in the reference configuration $\boldsymbol{B}_R$, the primary unknown will be the Gateaux differential $\overset{\circ}{\boldsymbol{x}} = \equiv \overset{\circ}{\tilde{\boldsymbol{x}}}\ (\boldsymbol{Y}, t; \beta_s, \Delta\beta_s)$.

In this section, the shape sensitivity equilibrium equations and boundary conditions are developed. A weak form for the differential form of the shape sensitivity equilibrium equation is developed and the sensitivity deformation field computed. The driving force for applications like metal forming is due to the contact conditions at the die-workpiece interface and the effect of contact on the sensitivity deformation problem is described. In contrast to the direct deformation problem which was solved using an updated Lagrangian framework, we pose the sensitivity problem using a total Lagrangian formulation. The sensitivity deformation problem is developed on the reference configuration $\boldsymbol{B}_R$ i.e. we monitor material points that occupy a *fictitious* location $\boldsymbol{Y} \in \boldsymbol{B}_R$.

The shape derivative of the equilibrium equation results in the following equation (here $\boldsymbol{P}$ is the Piola-Kirchhoff stress):

$$\overline{\nabla_X \bullet \overset{\circ}{\boldsymbol{P}}} + \overset{\circ}{\boldsymbol{f}} = \mathbf{0} \quad \forall\ \boldsymbol{X} \in\ \boldsymbol{B}_\mathbf{0} \text{ and } \forall\ \mathbf{t} \in\ [\mathbf{0}, \mathbf{t_f}] \tag{15}$$

Neglecting body forces and after some algebra, the above equation is expressed as follows:

$$\nabla_Y\ \overset{\circ}{\boldsymbol{P}} \left[\boldsymbol{F}_R{}^{-T}\right] - \nabla_Y \boldsymbol{P}\left[\boldsymbol{L}_R{}^T \boldsymbol{F}_R{}^{-T}\right] = \mathbf{0} \tag{16}$$

A variational form of this equation can now be posed as:

$$\int_{\boldsymbol{B}_R} \left(\nabla_Y\ \overset{\circ}{\boldsymbol{P}} \left[\boldsymbol{F}_R{}^{-T}\right] - \nabla_Y \boldsymbol{P}\left[\boldsymbol{L}_R{}^T \boldsymbol{F}_R{}^{-T}\right]\right) \bullet \tilde{\boldsymbol{u}}\ dV_R = 0$$

where $\tilde{\boldsymbol{u}}$ is a kinematically admissible sensitivity deformation field expressed over the reference configuration $\boldsymbol{B}_R$.

Using integration by parts, one arrives at the following variational shape sensitivity problem for $\overset{\circ}{\hat{\boldsymbol{x}}}\ (\boldsymbol{X}, t)$ using a formulation based on the reference configuration $\boldsymbol{B}_R$:

$$\begin{aligned}
&\int_{\boldsymbol{B}_R} \overset{\circ}{\boldsymbol{P}}\ \boldsymbol{F}_R{}^{-T} \bullet \nabla_Y \tilde{\boldsymbol{u}} dV_R \\
&+ \int_{\boldsymbol{B}_R} \overset{\circ}{\boldsymbol{P}} \left[\nabla_Y \bullet \boldsymbol{F}_R{}^{-T}\right] \bullet \tilde{\boldsymbol{u}} dV_R \\
&- \int_{\partial \boldsymbol{B}_{n+1}} \frac{1}{\det \boldsymbol{F}_R} \left\{\left(\boldsymbol{F}\boldsymbol{L}_R \boldsymbol{F}^{-1}\right) \bullet (\boldsymbol{n} \otimes \boldsymbol{n})\right\} \hat{\boldsymbol{t}} \bullet \tilde{\boldsymbol{u}}\ dA_{n+1} \\
&= \int_{\boldsymbol{B}_R} \boldsymbol{P}\left[\nabla_Y \bullet (\boldsymbol{L}_R{}^T \boldsymbol{F}_R{}^{-T})\right] \bullet \tilde{\boldsymbol{u}}\ dV_R \\
&+ \int_{\boldsymbol{B}_R} \boldsymbol{P}\boldsymbol{L}_R{}^T \boldsymbol{F}_R{}^{-T} \bullet \nabla_Y \tilde{\boldsymbol{u}}\ dV_R + \\
&\int_{\partial \boldsymbol{B}_{n+1}} \frac{1}{\det \boldsymbol{F}_R} \left\{\overset{\circ}{\hat{\boldsymbol{t}}} - \left(\boldsymbol{F}\boldsymbol{L}_R \boldsymbol{F}^{-1}\right) \bullet (\boldsymbol{n} \otimes \boldsymbol{n}) \hat{\boldsymbol{t}}\right\} \bullet \tilde{\boldsymbol{u}} dA_{n+1}
\end{aligned}$$

for every admissible test function $\tilde{\boldsymbol{u}}$. In the above equation the quantity $\boldsymbol{L}_R$ is the driving force for the shape sensitivity problem. The *design* deformation gradient $\boldsymbol{F}_R$ is known a priori from the prescribed reference geometric mapping.

The primary unknown of the above variational problem is the Gateaux differential $\overset{\circ}{\tilde{\boldsymbol{x}}}$ $(\boldsymbol{Y}, t; \beta_s, \Delta\beta_s)$. Thus in order to obtain the final form of the variational shape sensitivity problem, the relationship between $\overset{\circ}{\boldsymbol{F}}$ and $\overset{\circ}{\boldsymbol{x}}$ needs to be developed (refer to Figure 3). This takes the form:

$$\overset{\circ}{\boldsymbol{F}} = \left(\nabla_Y\ \overset{\circ}{\boldsymbol{x}}\right) \boldsymbol{F}_R{}^{-1} - \boldsymbol{F}\boldsymbol{L}_R \tag{17}$$

Taking $\boldsymbol{F}_R = \boldsymbol{I}$ in the variational equation above, results in the following simplified equation:

$$\begin{aligned}
&\int_{\boldsymbol{B}_0} \overset{\circ}{\boldsymbol{P}} \bullet \nabla_X \tilde{\boldsymbol{u}}\ dV_0 - \\
&\int_{\partial \boldsymbol{B}_{n+1}} \left\{\left(\overset{\circ}{\boldsymbol{F}}\ \boldsymbol{F}^{-1}\right) \bullet\ (\boldsymbol{I} - \boldsymbol{n} \otimes \boldsymbol{n})\right\} \hat{\boldsymbol{t}} \bullet \tilde{\boldsymbol{u}}\ dA_{n+1} = \\
&\int_{\boldsymbol{B}_0} \left(\boldsymbol{P}\left[\nabla_X \bullet \boldsymbol{L}_R^T\right]\right) \bullet \tilde{\boldsymbol{u}}\ dV_0 + \\
&\int_{\boldsymbol{B}_0} \left(\boldsymbol{P}\boldsymbol{L}_R^T\right) \bullet \nabla_X \tilde{\boldsymbol{u}}\ dV_0 + \\
&\int_{\partial \boldsymbol{B}_{n+1}} \left(\overset{\circ}{\hat{\boldsymbol{t}}} - \left(\boldsymbol{F}\boldsymbol{L}_R \boldsymbol{F}^{-1} \bullet\ (\boldsymbol{n} \otimes \boldsymbol{n})\right) \hat{\boldsymbol{t}}\right) \bullet \tilde{\boldsymbol{u}}\ dA_{n+1}
\end{aligned}$$

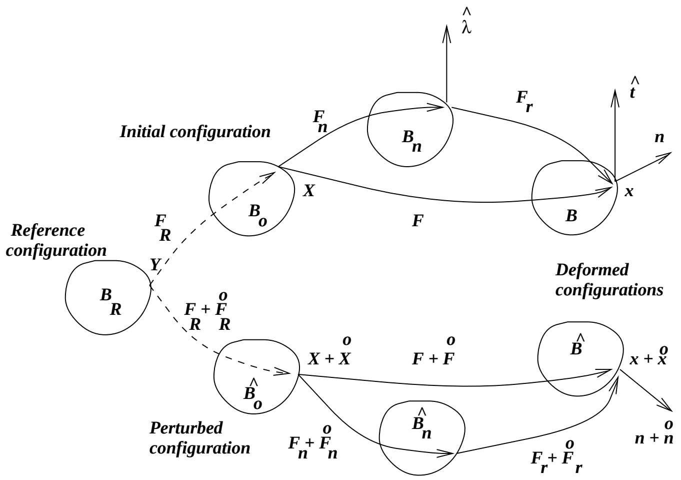

Figure 4: Schematic of the deformation history of a body corresponding to two nearby initial preforms.

In this case equation (17) takes the form :

$$\overset{\circ}{\boldsymbol{F}} = \overline{\nabla_X \overset{\circ}{\boldsymbol{x}}} = \nabla_X \ \overset{\circ}{\boldsymbol{x}} \ - \boldsymbol{F}\boldsymbol{L}_R \tag{19}$$

The modified weak form given above can now be used to obtain a linear system solvable for $\overset{\circ}{\tilde{\boldsymbol{x}}}\ (\boldsymbol{Y} \equiv \boldsymbol{X}, t; \beta_s, \Delta\beta_s)$. The initial conditions and non-contact related boundary conditions for the above problem can easily be derived. Calculation of the boundary conditions that arise from the contact and frictional conditions is a non-trivial task mainly due to the non-differentiable nature of contact.

The traction vector $\hat{\boldsymbol{t}}$ refers to the current contact traction expressed per unit current area. The effect of contact on the finite deformation direct problem is presented in (Zabaras and Srikanth 1999), (Laursen and Simo 1991) and (Simo and Laursen 1992). We re-iterate that an updated Lagrangian approach is used to solve the equilibrium equations with the reference configuration being updated every time increment. As part of the solution procedure, the current contact traction $\hat{\boldsymbol{\lambda}}$ expressed per unit reference area (updated reference configuration) is also computed. Figure 4 shows the various configurations of the body during a deformation process for two different but nearby initial preforms.

The contact traction vectors $\hat{\boldsymbol{t}}$ and $\hat{\boldsymbol{\lambda}}$ are related as:

$$\hat{\boldsymbol{t}} = \hat{\boldsymbol{\lambda}} \ \frac{|\boldsymbol{F}_r^T \boldsymbol{n}|}{J_r} \tag{20}$$

where $\boldsymbol{F}_r = \boldsymbol{F} \ \boldsymbol{F}_n^{-1}$ is the relative deformation gradient and $J_r = det\boldsymbol{F}_r$. One can thus modify the weak shape sensitivity problem given earlier as follows (where here $\boldsymbol{\partial B}_n$ is the part of the boundary where contact occurs):

$$\int_{\boldsymbol{B}_0} \overset{\circ}{\boldsymbol{P}} \bullet \nabla_X \tilde{\boldsymbol{u}} \, dV_0 +$$
$$\int_{\boldsymbol{\partial B}_n} \left\{ \overset{\circ}{\boldsymbol{F}} \left(\boldsymbol{F}^{-1} - \frac{\boldsymbol{F}_n^{-1} \boldsymbol{F}_r^T}{|\boldsymbol{F}_r^T \boldsymbol{n}|^2} \right) \bullet (\boldsymbol{n} \otimes \boldsymbol{n}) \right\} \hat{\boldsymbol{\lambda}} \bullet \tilde{\boldsymbol{u}} \, dA_n =$$
$$\int_{\boldsymbol{B}_0} \left(\boldsymbol{P} \left[\nabla_X \bullet \boldsymbol{L}_R^T \right] \right) \bullet \tilde{\boldsymbol{u}} \, dV_0 +$$
$$\int_{\boldsymbol{B}_0} \left(\boldsymbol{P} \boldsymbol{L}_R^T \right) \bullet \nabla_X \tilde{\boldsymbol{u}} \, dV_0 + \int_{\boldsymbol{\partial B}_n} \overset{\circ}{\hat{\boldsymbol{\lambda}}} \bullet \tilde{\boldsymbol{u}} \, dA_n +$$
$$\int_{\boldsymbol{\partial B}_n} \left(\frac{(\boldsymbol{F}_r \boldsymbol{F}_r^T) \bullet (\overset{\circ}{\boldsymbol{n}} \otimes \boldsymbol{n})}{|\boldsymbol{F}_r^T \boldsymbol{n}|^2} \right) \hat{\boldsymbol{\lambda}} \bullet \tilde{\boldsymbol{u}} \, dA_n +$$
$$\int_{\boldsymbol{\partial B}_n} \mathrm{tr} \left(\boldsymbol{F}_r \ \overset{\circ}{\boldsymbol{F}}_n \ \boldsymbol{F}^{-1} \right) \hat{\boldsymbol{\lambda}} \bullet \tilde{\boldsymbol{u}} \, dA_n$$
$$- \int_{\boldsymbol{\partial B}_n} \left(\frac{\boldsymbol{F}_r \overset{\circ}{\boldsymbol{F}}_n \boldsymbol{F}_n^{-1} \boldsymbol{F}_r^T}{|\boldsymbol{F}_r^T \boldsymbol{n}|^2} \right) \bullet (\boldsymbol{n} \otimes \boldsymbol{n}) \ \hat{\boldsymbol{\lambda}} \bullet \tilde{\boldsymbol{u}} \, dA_n -$$
$$\int_{\boldsymbol{\partial B}_n} \left(\boldsymbol{F} \boldsymbol{L}_R \boldsymbol{F}^{-1} \bullet (\boldsymbol{n} \otimes \boldsymbol{n}) \right) \hat{\boldsymbol{\lambda}} \bullet \tilde{\boldsymbol{u}} \, dA_n$$

The calculation of $\overset{\circ}{\hat{\boldsymbol{\lambda}}}$ must be consistent with the presentation of the direct deformation contact sub-problem. In the direct deformation problem, contact and friction conditions are calculated using an implicit augmented Lagrangian approach (Zabaras and Srikanth 1999). To address the issue of non-differentiability of the contact/frictional conditions, the following *regularizing assumptions* are made in the computation of the sensitivities of the contact tractions:

- Contact assumption: A particle that lies in the admissible (inadmissible) region at time t for a problem also lies in the admissible (inadmissible) region for a perturbed problem (i.e. for a deformation that results from a perturbed preform configuration) at time t.

- Friction assumption: Transition from stick to slip condition or vice versa does not occur at a material point as a result of a perturbation to the preform configuration.

Figure 5 shows the schematic used to compute the contact traction sensitivities. A scheme is developed to compute $\overset{\circ}{\hat{\boldsymbol{\lambda}}}$. The sensitivity of the closest point projection $\overset{\circ}{\boldsymbol{y}}$ plays a crucial role in the computation of the traction sensitivities. The contact traction vector is expressed from the descrip-

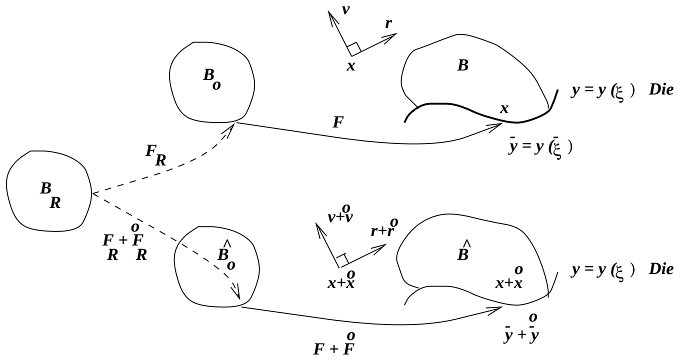

Figure 5: Schematic depicting the contact sensitivity sub-problem for changes in the preform shape.

tion of the direct deformation problem as (Zabaras and Srikanth 1999):

$$\boldsymbol{\lambda} = \lambda_N \; \boldsymbol{\nu}(\bar{\boldsymbol{y}}) \;-\; \lambda_T \; \boldsymbol{\tau}_1(\bar{\boldsymbol{y}}) \tag{21}$$

One obtains the sensitivity of the contact traction as:

$$\mathring{\boldsymbol{\lambda}} = \mathring{\lambda}_N \;\; \boldsymbol{\nu}(\bar{\boldsymbol{y}}) + \lambda_N \; \mathring{\boldsymbol{\nu}} \;-\; \mathring{\lambda}_T \;\; \boldsymbol{\tau}_1(\bar{\boldsymbol{y}}) \;-\; \lambda_T \; \mathring{\boldsymbol{\tau}}_1 \tag{22}$$

The variables $(\mathring{\boldsymbol{\lambda}}_n, \mathring{\bar{\xi}}_n)$ are assumed to be known as calculated from the solution of the contact sensitivity problem from the previous time-step. The solution of the direct deformation problem also gives the following variables at time t_{n+1}, $(\boldsymbol{\lambda}_N, \Phi^{trial}, \boldsymbol{\lambda}_T^{trial})$. The sensitivity of the trial state at time t_{n+1} is given as :

$$\mathring{\lambda}_N = \overline{\langle \lambda_{N_n} + \epsilon_N \; g(\boldsymbol{x}_{n+1}) \rangle}^{\circ} \tag{23}$$

$$\mathring{\lambda}_T^{trial} = \mathring{\lambda}_{T_n} \; + \epsilon_T \left(\mathring{\bar{\xi}} - \mathring{\bar{\xi}}_n \right) \tag{24}$$

As a result of the contact regularizing assumption, one can express the sensitivity of normal traction for points in contact as:

$$\mathring{\lambda}_N = \mathring{\lambda}_{N_n} + \epsilon_N \;\; \overline{g(\boldsymbol{x}_{n+1})}^{\circ} \tag{25}$$

The sensitivity of the tangential traction is given as (see friction related assumption):

$IF \;\; (\; \Phi^{trial} \leq 0 \;) \;\; THEN$

$$\mathring{\lambda}_T = \mathring{\lambda}_T^{trial} \quad (stick) \tag{26}$$

ELSE

$$\mathring{\lambda}_T = \overline{\left(\mu \; \lambda_N \; \frac{\lambda_T^{trial}}{\left\| \boldsymbol{\lambda}_T^{trial} \right\|} \right)}^{\circ} \quad (slip) \tag{27}$$

If the material point being analyzed is in sticking contact, then the sensitivity of the tangential traction $\mathring{\lambda}_T$ is obtained from the sensitivity of the trial state in equation (24). If however the friction conditions at a material point are that of slip, equation (27) is used to compute the sensitivity of the tangential traction.

With a number of steps and after calculating the linear relationship between the sensitivity of the gap function $\mathring{g}$ and $\mathring{\boldsymbol{x}}$, the sensitivity of the contact traction $\mathring{\boldsymbol{\lambda}}$ can be written as a known linear function of $\mathring{\boldsymbol{x}}$. With the substitution of this linear equation to the weak form, one has posed the entire shape sensitivity problem in an infinite dimensional setting along with all the necessary initial and boundary conditions (Srikanth and Zabaras 1999b).

As discussed earlier, an augmented Lagrangian formulation is used in the direct contact algorithm similar to that given in (Laursen and Simo 1991) and (Simo and Laursen 1992). Solution of the direct deformation problem within a time increment usually requires a number of augmentations in order to accurately enforce the various constraints. A sensitivity contact algorithm resulting from the differentiation of the discrete direct contact algorithm will lead to an iterative sensitivity contact subproblem. Such iterations however will not be consistent with the linear nature of the sensitivity analysis. The use of the same undersized penalties as those used in the direct deformation problem would result in significantly inaccurate estimates of sensitivities if only one iteration is performed in the contact sensitivity problem. This issue is addressed in (Srikanth and Zabaras 1999) where the use of much higher penalties for the sensitivity contact problem are proposed than those used in the direct contact subproblem. Such a choice of the penalty parameters prevents the need for additional iterations and results in very accurate measures of the sensitivity contact tractions (Srikanth and Zabaras 1999). The regularizing contact and frictional assumptions are responsible for this future of the augmented Lagrangian analysis since in the case of the sensitivity contact algorithm one calculates the sensitivities of the contact tractions while keeping the slip/stick contact boundaries fixed.

2.2 Open issues in the design of forming processes

There are many technical issues that remain to be addressed in the design and control of forming processes. Some of these issues of importance to our research are the following:

- The calculation of the sensitivities of the contact tractions remains a challenging unsolved problem. An algorithm is required that in addition to the calculation of the sensitivities of the contact tractions can also provide the sensitivities of the contact regions. An algorithm is needed with the minimum regularizing a-priori contact assumptions that is guaranteed to lead to unique, stable and accurate contact traction solutions.

- Initial designs are required based on ideal forming paths or microstructure evolution paths. Efficient algorithms for the development of realistic initial designs are not available yet for bulk forming processes.

- Consideration of constraint optimization problems for metal forming design are required. Some of these constrained problems may be handled as multiple stage designs.

- The design of multistage processes (i.e. the calculation of the sequence of processes that lead an initial workpiece to a desired product) is one of the remaining challenging problems in optimization theory.

- Design of processes that lead to a desired texture in the final product is a challenging open problem. First principle assumptions are required from passing sensitivity data between scales (i.e. the sensitivity of the deformation gradient).

5 ACKNOWLEDGEMENTS

Owen Richmond's impact in all aspects of our work is apparent. We dedicate these research efforts to him and we only hope that our work contributes to his long dream of integration of material, product and process design.

The work reported here has been supported by the National Science Foundation (DMII-9522613) and Alcoa Laboratories. The contributions of George Yang, Rajiv Sampath, Akkaram Srikanth and Yangang Bao in various aspects of the work presented here are appreciated.

5 REFERENCES

Badrinarayanan S., A. Constantinescou & N. Zabaras 1995. Preform design in metal forming. In: S.-F. Shen & P. Dawson (edts.), *Numiform'95: Simulation of Materials Processing: Theory, Meth. and Applications*:533-538. Rotterdam:Balkema.

Badrinarayanan, S. & N. Zabaras 1996. A sensitivity analysis for the optimal design of metal forming processes. *Comp. Meth. Appl. Mech. Engr.* 129:319–348.

Chung S.H. & S.M. Hwang 1998. Optimal process design in non-isothermal non-steady metal forming by the finite element method. *Int. J. Num. Meth. Engr.* 42:1343–1390.

Coriell, S.R. & G. B. McFadden, Morphological stability. In D.T.J. Hurle (ed.), *Handbook of Crystal Growth, Fundamentals: Transport and Stability.* 1b:785–857.

Flemings, M.C. 1974. *Solidification Processing.* New York: McGraw Hill.

Fletcher, R. 1987. *Practical Methods of Optimization.* Wiley: New York.

Fourment L. & J.L. Chenot 1996. Optimal design for non-steady state metal forming processes - I. Shape optimization method. *Int. J. Num. Meth. in Engr.* 39:33–50.

Fourment L., T. Balan & J.L. Chenot 1996. Optimal design for non-steady state metal forming processes - II. Application of shape optimization in forging. *Int. J. Num. Meth. Engr.* 39:51–65.

Joun M.S. & S.M. Hwang 1998. Die shape optimal design in three dimensional shape metal extrusion by the finite element method. *Int. J. Num. Meth. Engr.* 41:311–335.

Kang, S. & N. Zabaras 1995. Control of the freezing interface motion in two-dimensional solidification processes using the adjoint method. *Int. J. Num. Meth. Engr.* 38:63–80.

Kleiber M., H. Antúnez, T.D. Hien & P. Kowalczyk 1997. *Parameter Sensitivity in Nonlinear Mechanics: Theory and Finite Element Computations.* New York:Wiley.

Kobayashi S., S. Oh & T. Altan 1989. *Metal forming and the finite-element mothod.* New York:Oxford University Press.

Kurz, W. & D.J. Fisher 1989. *Fundamentals of Solidification.* Switzerland: Trans Tech Publ.

Laursen, T.A. & J.C. Simo 1991. On the formulation and Num. treatment of finite deformation frictional contact problems. In: P. Wriggers & W. Wager (edts.), *Nonlinear Comp. Mech. - State of the Art*: 716–736. Berlin: Springer.

Sampath, R. & N. Zabaras, in press. An object oriented implementation of a front tracking FEM for directional solidification processes. *Int. J. Num. Meth. Engr.*

Sampath, R. & N. Zabaras, submitted. Inverse thermal design and control of solidification processes in the presence of a strong external magnetic field. *J. Comput. Physics.*

Sampath, R. & N. Zabaras, submitted. An object-oriented implementation of adjoint techniques for the design of complex continuum systems. *Int. J. Num. Meth. Engr.*

Series, R.W. & D.T.J. Hurle 1991. The use of magnetic fields in semiconductor crystal growth. *J. Cryst. Growth.* 113:305-328

Simo, J.C. & T.A. Laursen 1992. An augmented Lagrangian treatment of contact problems involving friction. *Computers and Structures.* 42(1):97-116.

Srikanth, A. & N. Zabaras, submitted. Preform design and shape optimization in metal forming. *Comp. Meth. Appl. Mech. Engr.*

Weber, G. & L. Anand 1990. Finite deformation constitutive equations and a time integration procedure for isotropic, hyperelastic -viscoplastic solids. *Comp. Meth. Appl. Mech. Engr.* 79:173–202.

Yang, G.Z. & N. Zabaras 1998a. An adjoint method for the inverse design of solidification processes with natural convection *Int. J. Num. Meth. Engr.* 42:1121–1144.

Yang, G.Z. & N. Zabaras 1998b. The adjoint method for an inverse design problem in the directional solidification of binary alloys. *J. Comput. Physics.* 140:432–452.

Zabaras, N., S. Mukherjee & O. Richmond 1988. An analysis of inverse heat transfer problems with phase changes using an integral method. *J. of Heat Transfer ASME.* 110:554–561.

Zabaras, N., Y. Ruan & O. Richmond 1992. On the design of two-dimensional Stefan processes with desired freezing front motions. *Num. Heat Transfer.* 21B:307–325.

Zabaras, N. & S. Kang 1993. On the solution of an ill-posed inverse design solidification problem using minimization techniques in finite and infinite dimensional spaces. *Int. J. Num. Meth. Engr.* 36:3973–3990.

Zabaras, N. & T. Hung Nguyen 1995. Control of the freezing interface morphology in solidification processes in the presence of natural convection. *Int. J. Num. Meth. Engr.* 38:1555–1578.

Zabaras, N. & G. Yang, 1997. A functional optimization and implementation for an inverse natural convection problem. *Comp. Meth. Appl. Mech. Engr.* 144:245–274.

Zabaras, N. 1998. Adjoint Meth. for inverse free convection problems with application to solidification processes. In J. Borggaard, E. Cliff, S. Schreck & J. Burns (edts.), *Computational Methods for Optimal Design and Control.* Series in Progress in Systems and Control Theory:391–426. New York:Birkhauser.

Zabaras, N. & Y. Bao, submitted. A continuum sensitivity analysis for metal forming processes with application to die design problems. *Int. J. Num. Meth. Engr.*

Zabaras, N. & A. Srikanth, in press. An object oriented programming approach to the Lagrangian FEM analysis of large inelastic deformations and metal forming processes. *Int. J. Num. Meth. Engr.*

Zhao G., E. Wright & R.V. Grandhi 1997. Preform Die shape design in metal forming using an optimization method. *Int. J. Num. Meth. Engr.* 40:1213-1230.

Zhou, K., J.C. Doyle & K. Glover 1996. *Robust and Optimal Control.* New Jersey:Prentice Hall.